Ghost imaging with incoherent and partially coherent light radiation

Yangjian Cai[1,2] and Shi-Yao Zhu[1,2]
[1]*Department of Physics, Hong Kong Baptist University, Hong Kong, China*
[2]*Institute of Optics, Department of Physics, ZheJiang University, Hangzhou, 310027, China*
(Received 17 August 2004; revised manuscript received 28 February 2005; published 17 May 2005)

We theoretically study ghost imaging with incoherent and partially coherent light radiation by using classical optical coherence theory. A Gaussian thin lens equation is derived for the ghost image. The equation depends on both paths. The quality and visibility of the ghost image are influenced by the source's transverse size, coherence width, and object characteristics. The differences between ghost imaging formed with incoherent light radiation and with entangled photon pairs are discussed.

DOI: 10.1103/PhysRevE.71.056607 PACS number(s): 42.30.Va, 42.25.Kb, 42.25.Hz

I. INTRODUCTION

Ghost imaging and interference were first realized by using entangled photon pairs generated in spontaneous parametric down-conversion in 1995 [1,2]. The name "ghost" comes from the fact that an object in one path produces an image or interference fringes in another path in the measurement of coincident counting rates, and the image or fringes depend on both paths. Since then, many theoretical and experimental studies on this subject have been published [3–12], due to their great potential applications in quantum metrology, lithography, and holography [13–18]. Recently, there have been discussions about whether quantum entanglement is necessary in ghost imaging and interference and whether the ghost imaging and interference can be realized with classical source [19–25]. Bennink *et al.* presented their classical ghost imaging and interference experiments using classical coherent light [20,21]. Furthermore, Angelo and Shih [22] claimed that the classical coherent ghost image is just a shot-by-shot, point-to-point projection. Gatti *et al.* first pointed out theoretically that the ghost imaging can be achieved with truly incoherent light [23,24]. Cheng and Han studied the coincidence interference with a complete incoherent light and without any lens (similar scheme with the quantum ghost interference) from classically theory [25]. Recently, Valencia *et al.* demonstrated experimentally ghost imaging with quasi-thermal light [26], and almost at the same time, Magatti *et al.* realized ghost imaging and ghost diffraction with classical quasi-thermal light in an experiment [27]. We have studied the ghost interference formed with partially coherent light radiation [28]. In this paper, we present a theoretical study of the ghost imaging formed with incoherent and partially coherent light radiation, and investigate the visibility and quality of the image using classically optical coherence theory. The similarities and differences of the ghost imaging formed with incoherent light and with entangled photon pairs are discussed.

II. GHOST IMAGING EQUATION

The scheme for the ghost imaging with incoherent light radiation is shown Fig. 1. The incoherent light first was split by a beam splitter and then propagates through paths 1 and 2 to detectors 1 and 2, respectively. In path 1, between the beam splitter and detector 1, there is an object (maybe a double slit) with transmission function $H(v)$. In path 2, there is a lens with focal length f between the beam splitter and detector 2, and the distance between the source and detector 2 is divided into l_1 and l_2. The coincident counting rate is proportional to the second order correlation function $G^{(2)}(u_1,u_2)$.

According to optical coherence theory, the second order correlation function between the detectors obeys the following integral formula for the incoherent light [23,24]:

$$\begin{aligned} G^{(2)}(u_1,u_2) &= \langle E(u_1)E(u_2)E^*(u_2)E^*(u_1)\rangle \\ &= \int_{-\infty}^{\infty}\int_{-\infty}^{\infty}\int_{-\infty}^{\infty}\int_{-\infty}^{\infty} h_1(x_1,u_1)h_1^*(x_4,u_1) \\ &\quad \times h_2(x_2,u_2)h_2^*(x_3,u_2)\langle E(x_1)E(x_2)E^*(x_3) \\ &\quad \times E^*(x_4)\rangle dx_1dx_2dx_3dx_4 \\ &= \langle I(u_1)\rangle\langle I(u_2)\rangle + |\Gamma(u_1,u_2)|^2, \end{aligned} \tag{1}$$

where $E(x)$ and $E(u)$ are the electric fields of the light in the source plane and in the detection plane, respectively. $h_1(x_1,u_1)$ and $h_2(x_2,u_2)$ are the response functions of the two paths through which the radiation light passes, and

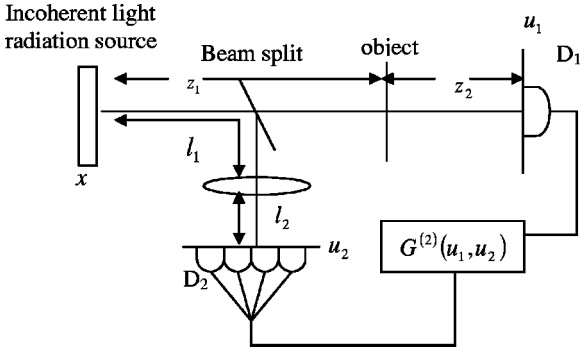

FIG. 1. The scheme for ghost imaging with incoherent light radiation with the lens in path 2.

$$\langle I(u_i)\rangle = \int_{-\infty}^{\infty}\int_{-\infty}^{\infty} h_i(x_1,u_i)h_i^*(x_2,u_i)\langle E(x_1)E^*(x_2)\rangle dx_1dx_2, \quad i=1,2, \tag{2}$$

$$\Gamma(u_1,u_2) = \int_{-\infty}^{\infty}\int_{-\infty}^{\infty}\langle E(x_1)E^*(x_2)\rangle h_1(x_1,u_1)h_2^*(x_2,u_2)dx_1dx_2. \tag{3}$$

Here $\langle I(u_i)\rangle$ is the first order correlation function at the same space point (the intensity at the ith detector), and depends only on the ith path, while $\Gamma(u_1,u_2)$ is the first order cross correlation function at two different points, which is related to both detectors and depends on both paths. $\langle I(u_1)\rangle, \langle I(u_2)\rangle$, and $\Gamma(u_1,u_2)$ have contributions to the coincident counting rates. To obtain Eq. (1), the source field fluctuations have been assumed to be a Gaussian random process and to obey Gaussian statistics. Equations (2) and (3) are valid for optical systems under the condition of linearly shift invariance and paraxial regime.

The first order correlation function for a completely incoherent source can be expressed as

$$\langle E(x_1)E^*(x_2)\rangle = I(x_1)\delta(x_1-x_2), \tag{4}$$

where $I(x_1)$ is the intensity distribution of the source. In this section we assume that the source's size is infinite and the intensity distribution is uniform, and then $I(x_1)$ can be expressed as a constant I_0.

With the help of Collins' formula, which is the generalized Fresnel integral formula for treating the light propagating through complex optical system by use of a convenient matrix method [29], we can obtain detailed information about the two paths $h_1(x_1,u_1)$ and $h_2(x_2,u_2)$. Substituting them into Eqs. (1)–(3), we obtain

$$\begin{aligned}\langle I(u_1)\rangle &= \frac{I_0}{\lambda^2 z_1 z_2}\int_{-\infty}^{\infty}\int_{-\infty}^{\infty}\int_{-\infty}^{\infty}\int_{-\infty}^{\infty}\delta(x_1-x_2)\\ &\times\exp\left[-\frac{i\pi}{\lambda z_1}(x_1^2-2x_1v_1+v_1^2)\right]\\ &\times\exp\left[\frac{i\pi}{\lambda z_1}(x_2^2-2x_2v_2+v_2^2)\right]H(v_1)H^*(v_2)\\ &\times\exp\left[-\frac{i\pi}{\lambda z_2}(v_1^2-2v_1u_1+u_1^2)\right]\\ &\times\exp\left[\frac{i\pi}{\lambda z_2}(v_2^2-2v_2u_1+u_1^2)\right]dx_1dx_2dv_1dv_2\\ &= \frac{I_0}{\lambda z_2}\int_{-\infty}^{\infty}|H(v_1)|^2dv_1 = \text{const},\end{aligned} \tag{5}$$

$$\begin{aligned}\langle I(u_2)\rangle &= \frac{I_0}{\lambda b_2}\int_{-\infty}^{\infty}\int_{-\infty}^{\infty}\delta(x_1-x_2)\\ &\times\exp\left[-\frac{i\pi}{\lambda b_2}(a_2x_1^2-2x_1u_2+d_2u_2^2)\right]\\ &\times\exp\left[\frac{i\pi}{\lambda b_2}(a_2x_2^2-2x_2u_2+d_2u_2^2)\right]dx_1dx_2\\ &= \frac{I_0}{\lambda b_2}\int_{-\infty}^{\infty}dx_1 = \infty,\end{aligned} \tag{6}$$

$$\begin{aligned}|\Gamma(u_1,u_2)|^2 &= \frac{I_0^2}{\lambda^3 z_1 z_2|b_2|}\left|\int_{-\infty}^{\infty}\int_{-\infty}^{\infty}\int_{-\infty}^{\infty}\delta(x_1-x_2)H(v_1)\right.\\ &\times\exp\left[-\frac{i\pi}{\lambda z_1}(x_1^2-2x_1v_1+v_1^2)\right.\\ &\left.-\frac{i\pi}{\lambda z_2}(v_1^2-2v_1u_1+u_1^2)\right]\\ &\left.\times\exp\left[\frac{i\pi}{\lambda b_2}(a_2x_2^2-2x_2u_2+d_2u_2^2)\right]dx_1dx_2dv_1\right|^2\\ &= \frac{I_0^2}{\lambda^3 z_1 z_2|b_2|}\left|\int_{-\infty}^{\infty}\int_{-\infty}^{\infty}H(v_1)\right.\\ &\times\exp\left[-\frac{i\pi}{\lambda z_1}(x_1^2-2x_1v_1+v_1^2)\right.\\ &\left.-\frac{i\pi}{\lambda z_2}(v_1^2-2v_1u_1+u_1^2)\right]\\ &\left.\times\exp\left[\frac{i\pi}{\lambda b_2}(a_2x_1^2-2x_1u_2+d_2u_2)\right]dx_1dx_2dv_1\right|^2,\end{aligned} \tag{7}$$

where a_2, b_2, c_2, and d_2 are the optical transfer matrix elements between the light source and detector 2,

$$\begin{aligned}\begin{pmatrix}a_2 & b_2\\ c_2 & d_2\end{pmatrix} &= \begin{pmatrix}1 & l_2\\ 0 & 1\end{pmatrix}\begin{pmatrix}1 & 0\\ -1/f & 1\end{pmatrix}\begin{pmatrix}1 & l_1\\ 0 & 1\end{pmatrix}\\ &= \begin{pmatrix}1-\frac{l_2}{f} & l_1+l_2-\frac{l_1l_2}{f}\\ -\frac{1}{f} & 1-\frac{l_1}{f}\end{pmatrix}.\end{aligned} \tag{8}$$

If we set the Gaussian thin lens equation in Eq. (8),

$$\frac{1}{l_1-z_1}+\frac{1}{l_2}=\frac{1}{f}, \tag{9}$$

we have

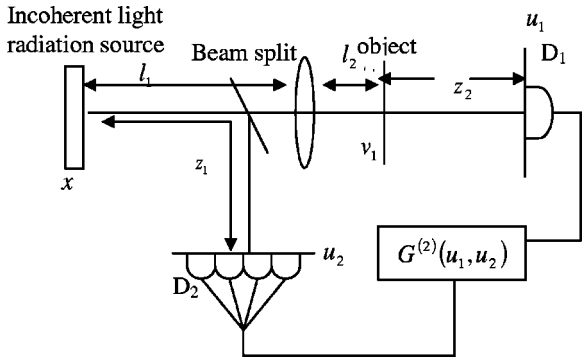

FIG. 2. The scheme for ghost imaging with incoherent light radiation with the lens in path 1.

$$\begin{pmatrix} a_2 & b_2 \\ c_2 & d_2 \end{pmatrix} = \begin{pmatrix} 1 & l_2 \\ 0 & 1 \end{pmatrix} \begin{pmatrix} 1 & 0 \\ -\dfrac{1}{l_1 - z_1} - \dfrac{1}{l_2} & 1 \end{pmatrix} \begin{pmatrix} 1 & l_1 \\ 0 & 1 \end{pmatrix} = \begin{pmatrix} -\dfrac{l_2}{l_1 - z_1} & -\dfrac{z_1 l_2}{l_1 - z_1} \\ -\dfrac{1}{l_2} - \dfrac{1}{l_1 - z_1} & 1 - \dfrac{l_1}{l_2} - \dfrac{l_1}{l_1 - z_1} \end{pmatrix}. \quad (10)$$

Substituting Eq. (10) into Eq. (7), we obtain

$$\begin{aligned} |\Gamma(u_1,u_2)|^2 &= \frac{I_0^2}{\lambda^3 z_1 z_2 |b_2|} \left| \int_{-\infty}^{\infty} \int_{-\infty}^{\infty} H(v_1) \exp\left[\frac{2i\pi}{\lambda z_1}\left(v_1 - \frac{u_2}{a_2}\right) x_1 \right.\right. \\ &\quad \left.\left. - \frac{i\pi}{\lambda z_1} v_1^2 - \frac{i\pi}{\lambda z_2}(v_1^2 - 2v_1 u_1) \right] dx_1 dv_1 \right|^2 \\ &= \frac{I_0^2}{\lambda z_2 |a_2|} \left| \int_{-\infty}^{\infty} \delta\left(v_1 - \frac{u_2}{a_2}\right) H(v_1) \right. \\ &\quad \left. \times \exp\left[-\frac{i\pi}{\lambda z_1} v_1^2 - \frac{i\pi}{\lambda z_2}(v_1^2 - 2v_1 u_1) \right] dv_1 \right|^2 \\ &= \frac{I_0^2}{\lambda z_2 |a_2|} \left| H\left(\frac{u_2}{a_2}\right) \right|^2, \end{aligned} \quad (11)$$

where the integral formula $(1/2\pi)\int_{-\infty}^{\infty}\exp(iqx)dx = \delta(q)$ has been used. It is clear that $\Gamma(u_1,u_2)$ represents the image of the object with an amplification of a_2.

Now we consider the case where the lens is located in path 1 (see Fig. 2), which is the same as the quantum image scheme in [2]. Similarly, by substituting Eq. (4) and detailed information about the two paths $h_1(x_1,u_1)$ and $h_2(x_2,u_2)$ into Eq. (3), we obtain

$$\begin{aligned} |\Gamma(u_1,u_2)|^2 &= \frac{I_0^2}{\lambda^3 z_1 z_2 |b_1|} \left| \int_{-\infty}^{\infty} \int_{-\infty}^{\infty} H(v_1) \exp\left[-\frac{i\pi}{\lambda b_1}(a_1 x_1^2 \right.\right. \\ &\quad \left. - 2x_1 v_1 + d_1 v_1^2) - \frac{i\pi}{\lambda z_2}(v_1^2 - 2v_1 u_1 + u_1^2) \right] \\ &\quad \left. \times \exp\left[\frac{i\pi}{\lambda z_1}(x_1^2 - 2x_1 u_2 + u_2) \right] dx_1 dx_2 dv_1 \right|^2, \end{aligned} \quad (12)$$

where a_1, b_1, c_1, and d_1 are the optical transfer matrix elements between the light source and detector 1,

$$\begin{pmatrix} a_1 & b_1 \\ c_1 & d_1 \end{pmatrix} = \begin{pmatrix} 1 & l_2 \\ 0 & 1 \end{pmatrix} \begin{pmatrix} 1 & 0 \\ -1/f & 1 \end{pmatrix} \begin{pmatrix} 1 & l_1 \\ 0 & 1 \end{pmatrix} = \begin{pmatrix} 1 - \dfrac{l_2}{f} & l_1 + l_2 - \dfrac{l_1 l_2}{f} \\ -\dfrac{1}{f} & 1 - \dfrac{l_1}{f} \end{pmatrix}. \quad (13)$$

If we set the Gaussian equation [Eq. (9)] in Eq. (13), and then substitute Eq. (13) into Eq. (12), we obtain

$$|\Gamma(u_1,u_2)|^2 = \frac{I_0^2 |a_1|}{\lambda z_2} |H(u_2 a_1)|^2, \quad (14)$$

which is the image of the object with an amplification of $1/a_1$.

From Eqs. (11) and (14), we find that $\Gamma(u_1,u_2)$ represents the ghost image of the object if the Gaussian lens equation (9) is satisfied, no matter whether the lens is located in path 1 or path 2.

Comparing the Gaussian lens equation Eq. (9) with the corresponding equations for the quantum ghost image [2], the following differences can be found. (1) l_1+z_1 in the imaging formation equation for the quantum case is replaced by l_1-z_1 for incoherent light radiation. (2) For $l_1>z_1$, we have an inverted and enlarged image with $l_2>2f$ or an inverted and reduced image with $2f>l_2>f$; for $l_1<z_1$, we have an erect and reduced image with $0<l_2<f$. The differences come from the classical and quantum nature of the correlation functions. In the quantum case, the cross correlation function is $\Gamma(x_1,x_2) \propto \langle 0,0|E(x_1)E(x_2)|\Psi\rangle$ due to the entanglement, while in the classical case (no entanglement) it is Eq. (3) where we have $E^*(x_2)$ instead of $E(x_2)$ and $h_1(x_1,u_1)h_2^*(x_2,u_2)$ instead of $h_1(x_1,u_1)h_2(x_2,u_2)$ [23,24]. The complex conjugate gives the minus sign in Eq. (9).

Assume the object to be a double slit whose transmission function is given by $H(v)=1$ for $-d/2-a/2<v<-d/2+a/2$ and $d/2-a/2<v<d/2+a/2$, and 0 otherwise, where a is the slit width and d is the slit distance of the two slits. In Fig. 3, we show how the image of the object (a double slit) is formed, when we vary l_2 from satisfying to not satisfying Eq. (9).

Equations (11) and (14) give perfect images of the object. However, the coincident counting rate is proportional to $G^{(2)}(u_1,u_2)$. Although the background $\langle I(u_1)\rangle\langle I(u_2)\rangle$ is a constant, it does not affect the quality of the image, but determines the visibility of the classical ghost image. We define the visibility of the image as

$$V = \frac{|\Gamma(u_1=0,u_2)|^2_{\max}}{G^{(2)}(u_1=0,u_2)_{\max}}. \quad (15)$$

From Eqs. (5) and (6), we can find that $\langle I(u_1)\rangle\langle I(u_2)\rangle=\infty$, that is to say, the visibility of the ghost image is zero. To have an observable ghost image, we need to consider how to

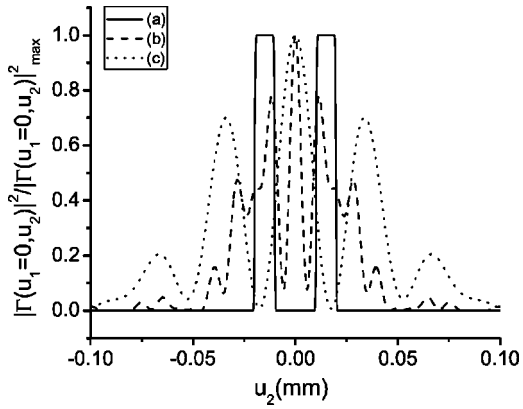

FIG. 3. The image pattern of a double slit with incoherent light for different l_2. (a) 20 (imaging case), (b) 20.5, and (c) 21.5 mm with $\lambda=702$ nm, $a=0.01$ mm, $d=0.03$ mm, $z_1=10$ mm, $z_2=40$ mm, $f=10$ mm, and $l_1=30$ mm.

increase the visibility while to keep good quality of the image, which can be realized by adjusting the size of the source, and/or the incoherence of the source.

III. THE FORMATION OF A VISIBLE GHOST IMAGE

In the above calculation and discussion, we have assumed the surface size of the light source to be infinite and the light source to be completely incoherent. In the practical case, completely incoherent light and infinite surface size do not exist. What are the influences of finite surface size and partial coherence on the quality and visibility of the ghost image?

We assume the light source to be a typical partially coherent source—a Gaussian Schell-model source. In this model the first order correlation function in the source plane can be expressed as [30]

$$\langle E(x_1)E^*(x_2)\rangle = G_0 \exp\left[-\frac{x_1^2+x_2^2}{4\sigma_I^2}-\frac{(x_1-x_2)^2}{2\sigma_g^2}\right], \quad (16)$$

where G_0 is a constant and set to unity in the following text, σ_I represents the source's transverse size, and σ_g is the source's transverse coherence width.

We only consider the case in which the lens is located in path 2 as shown in Fig. 1. Substituting Eq. (16) and detailed information about $h_1(x_1,u_1)$ and $h_2(x_2,u_2)$ into Eqs. (1)–(3), we obtain

$$\langle I(u_1=0)\rangle = \frac{\pi}{\lambda^2 z_1 z_2\sqrt{A_1A_2}}\int_{-\infty}^{\infty}\int_{-\infty}^{\infty} H(v_1)H^*(v_2) \times\exp\left[\frac{\left(\frac{2i\pi}{\lambda z_1}v_1-\frac{i\pi}{A_1\sigma_g^2\lambda z_1}v_2\right)^2}{4A_2}\right] \times\exp\left[-\frac{\pi^2}{A_1\lambda^2 z_1^2}v_2^2\right]\exp\left[-\frac{i\pi}{\lambda z_1}v_1^2-\frac{i\pi}{\lambda z_2}v_1^2\right] \times\exp\left[\frac{i\pi}{\lambda z_1}v_2^2+\frac{i\pi}{\lambda z_2}v_2^2\right]dv_1dv_2, \quad (17)$$

with

$$A_1=\frac{1}{4\sigma_I^2}+\frac{1}{2\sigma_g^2}-\frac{i\pi}{\lambda z_1}, \quad A_2=\frac{1}{4\sigma_I^2}+\frac{1}{2\sigma_g^2}+\frac{i\pi}{\lambda z_1}-\frac{1}{4A_1\sigma_g^4};$$

$$\langle I(u_2)\rangle = \frac{\pi}{\lambda|b_2|\sqrt{B_1B_2}}\exp\left[\frac{\left(\frac{2i\pi}{\lambda z_1}u_2-\frac{i\pi}{B_1\sigma_g^2\lambda b_2}u_2\right)^2}{4B_2}\right] \times\exp\left[-\frac{\pi^2}{B_1\lambda^2 b_2^2}u_2^2\right], \quad (18)$$

with

$$B_1=\frac{1}{4\sigma_I^2}+\frac{1}{2\sigma_g^2}-\frac{i\pi a_2}{\lambda b_2}, \quad B_2=\frac{1}{4\sigma_I^2}+\frac{1}{2\sigma_g^2}+\frac{i\pi a_2}{\lambda b_2}-\frac{1}{4B_1\sigma_g^4};$$

$$|\Gamma(u_1=0,u_2)|^2 = \frac{\pi^2}{\lambda^3 z_1 z_2|b_2|C_1C_2}\left|\int_{-\infty}^{\infty}H(v_1) \times\exp\left[\frac{\left(\frac{2i\pi}{\lambda z_1}v_1-\frac{i\pi}{C_1\sigma_g^2\lambda b_2}u_2\right)^2}{4C_2}\right] \times\exp\left[-\frac{\pi^2}{C_1\lambda^2 b_2^2}u_2^2\right]\exp\left[-\frac{i\pi}{\lambda z_1}v_1^2 -\frac{i\pi}{\lambda z_2}v_1^2\right]dv_1\right|^2, \quad (19)$$

with

$$C_1=\frac{1}{4\sigma_I^2}+\frac{1}{2\sigma_g^2}-\frac{i\pi a_2}{\lambda b_2}, \quad C_2=\frac{1}{4\sigma_I^2}+\frac{1}{2\sigma_g^2}+\frac{i\pi}{\lambda z_1}-\frac{1}{4C_1\sigma_g^4}.$$

Substituting Eqs. (9) and (10) into Eqs. (17)–(19), we can numerically study the ghost image formed with partially coherent light radiation. In Figs. 4 and 5 we show the normalized coincident counting for different transverse sizes and transverse coherence widths of the light source, respectively. The parameters for the following figures are $\lambda=702$ nm, $a=0.01$ mm, $d=0.03$ mm, $z_1=10$ mm, $z_2=40$ mm, $f=10$ mm, $l_1=30$ mm and $l_2=20$ mm. From Fig. 4, we can find that when σ_I increases, the quality of the image increases, while the visibility decreases. From Fig. 5, we can find that when σ_g decreases, the quality of the image increases, while the visibility decreases. Our results are coincident with the results of Refs. [23,24]. The coherence width of the source decides the resolution length of the imaging system; hence the resolution length increases with the increase of the coherence width, and while the image quality decreases. The coherence width is inversely proportional to the transverse size; thus the transverse size has opposite influences on the visibility and quality of the image [23,24].

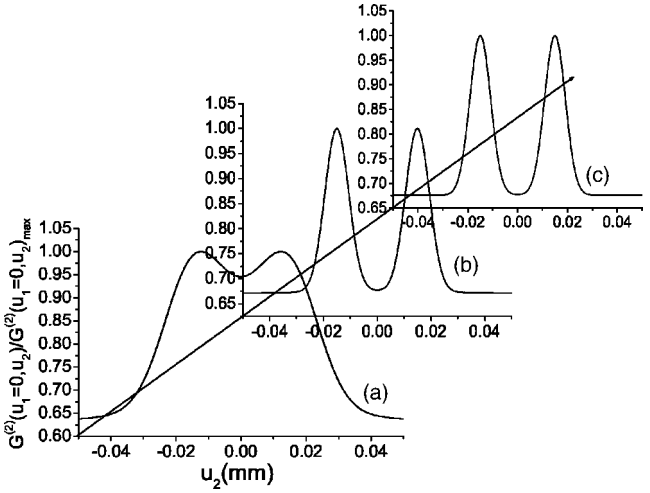

FIG. 4. The ghost images of a double slit aperture for different σ_l (a) 0.1, (b) 0.5, and (c) 5 mm with σ_g=0.005 mm.

Now we study the dependence of the visibility and quality of the image on the σ_g and σ_l in detail. We define a quality factor for the image,

$$Q = \frac{\int_{-\infty}^{\infty} \left| \frac{|\Gamma(u_1=0,u_2)|^2}{|\Gamma(u_1=0,u_2)|^2_{\max}} - \frac{|H(u_2)|^2}{|H(u_2)|^2_{\max}} \right| du_2}{\int_{-\infty}^{\infty} |H(u_2)|^2 du_2}. \quad (20)$$

A small Q value corresponds to high image quality. The dependences of the visibility and quality of the image of a double slit aperture on σ_g are shown in Figs. 6 and 7, respectively. It is clear from Figs. 6 and 7 that the visibility of the ghost image increases with decrease of σ_l or increase of σ_g, while the quality increases with the increase of σ_l or decrease of σ_g. High quality is accompanied by poor visibility, and good visibility accompanied by low quality. In order to observe the classical ghost image with partially coherent

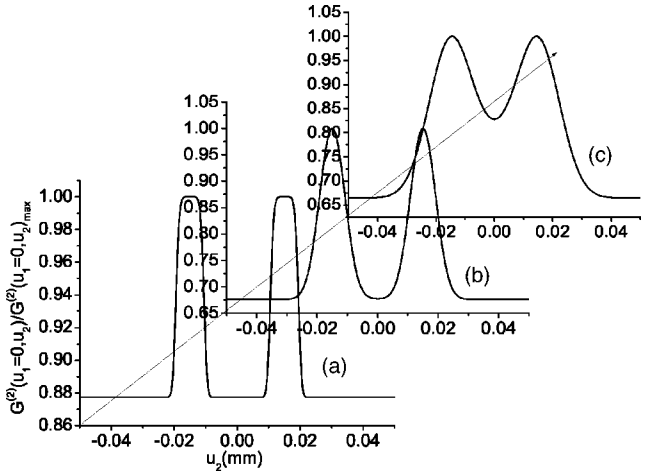

FIG. 5. The ghost images of a double slit aperture for different σ_g (a) 0.001, (b) 0.005, and (c) 0.01 mm with σ_l=5 mm.

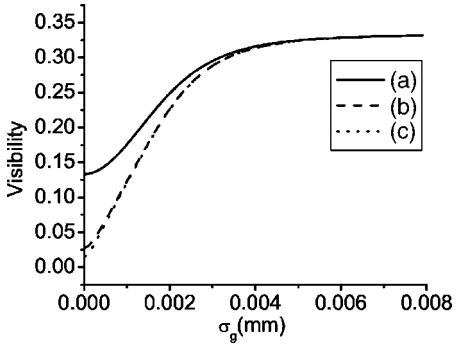

FIG. 6. Dependence of the visibility of the image of a double slit aperture versus σ_g for different σ_l: (a) 1, (b) 5, and (c) 10 mm.

light radiation, the selection of suitable transverse size and transverse coherence width is essential.

By comparing our result with that for the quantum ghost image [1,2,9], we find that in the quantum ghost image, good quality and high visibility can be achieved simultaneously [1,2], but it is impossible in a ghost image with incoherent light radiation. In the quantum case, the visibility and quality of the image are strongly influenced by the biphoton pump source; the narrower the size of the pump source, the more separable is the biphoton wave function and the less entangled is the field, and therefore the lower the visibility and worse quality of the ghost image [9]; while in the classical incoherent case, the visibility and quality of the image are controlled by the incoherent light radiation source, the narrower the size of the incoherent source, the more coherent is the light, and therefore the higher visibility and worse quality of the ghost image.

In the above calculations, we have assumed the object to be double slits. To learn about the influence of the object's features on the quality and visibility, in Fig. 8, we calculated the ghost images of different objects. It is clear from Fig. 8 that with the increase of the number of the slits (the object becomes more complex), the visibility of the image decreases, while the quality is not influenced. To learn about the influence of the slit width on the visibility of the image, in Fig. 9, we calculated the image of a slit with different slit

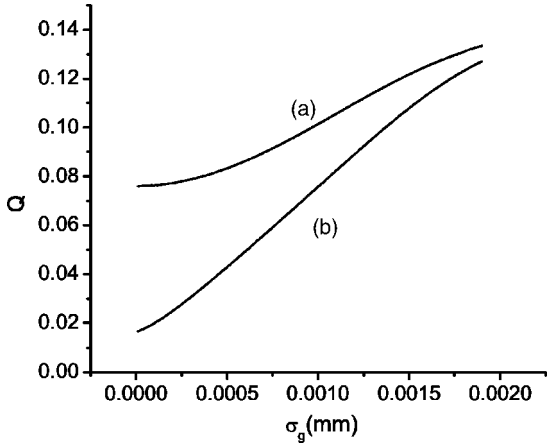

FIG. 7. Dependence of the quality of the image of a double slit aperture versus σ_g for different σ_l: (a) 1 and (b) 5 mm.

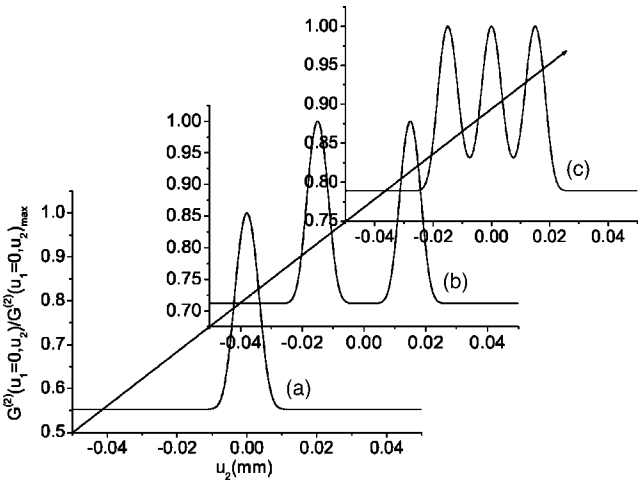

FIG. 8. The ghost images of different objects in the scheme of Fig. 1. (a) Single slit with slit width $a=0.01$ mm, (b) double slits with slit width $a=0.01$ mm, distance between two slits $d=0.03$ mm, (c) triple slits with slit width $a=0.01$ mm, distance between two nearby slits $d=0.015$ mm with $\lambda=702$ nm, $z_1=10$ mm, $z_2=40$ mm, $f=10$ mm, $l_1=30$ mm, $l_2=20$ mm, $\sigma_l=5$ mm, and $\sigma_g=0.003$ mm.

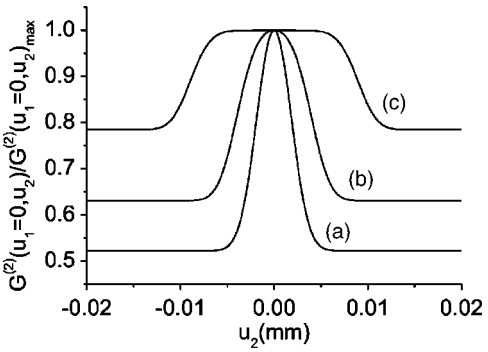

FIG. 9. The ghost images of a slit in the scheme of Fig. 1 for different slit widths a= (a) 0.005, (b) 0.01, and (c) 0.02 mm with $\lambda=702$ nm, $z_1=10$ mm, $z_2=40$ mm, $f=10$ mm, $l_1=30$ mm, $l_2=20$ mm, $\sigma_l=5$ mm, and $\sigma_g=0.002$ mm.

width. It is clear from Fig. 9 that the visibility of the slit decreases with the increase of the slit width. This indicates that the background $\langle I(u_1)\rangle\langle I(u_2)\rangle$ increases more rapidly than the cross correlation function $|\Gamma(x_1,x_2)|^2$ with the increase of the slit width or the number of the slits, which leads to a decrease of the visibility.

IV. CONCLUSIONS

Ghost imaging can be produced with incoherent and partially coherent light radiation. The equation for formation of the image is derived with some differences from that for the quantum image. The dependence of the quality and visibility on the two parameters the size (σ_l) and the coherence (σ_g) of the source are studied. The larger the surface (σ_l) is, the better the quality, and the smaller the visibility of the image. The larger the coherence between two points in the source plane (σ_g) is, the worse the quality, and the higher the visibility. Perfect imaging is impossible, because they are companied by zero visibility. In order to have observable visibility of the ghost image or interference fringes, we need to reduce the quality of the image (imperfect imaging) by choosing suitable size and coherence for the source. The visibility and the quality of the image also depend on the characteristics of the object or the slits (the number of the slits and width of the slits). The nature of the ghost imaging is due to the entanglement in quantum case and is due to the Hanbury-Brown-Twiss effect (low coherence with fluctuations but not completely no coherence) in the classical incoherent case.

In the above discussion, the temporal correlation time is assumed longer than the response time of the detectors. A partially coherent source with long coherence time can be produced from a laser beam scattered by rotated ground glass [24,26,27]. More recently, ghost image experiment with blackbody radiation was reported [31]; the blackbody radiation is a typical partial coherent radiation with high temperature corresponding to low coherence (small σ_g).

ACKNOWLEDGMENTS

This work was supported by RGC (Grant No. CA02/03.SC01) and FRG of Hong Kong Baptist University.

[1] D. V. Strekalov, A. V. Sergienko, D. N. Klyshko, and Y. H. Shih, Phys. Rev. Lett. **74**, 3600 (1995).
[2] T. B. Pittman, Y. H. Shih, D. V. Strekalov, and A. V. Sergienko, Phys. Rev. A **52**, R3429 (1995).
[3] P. H. S. Ribeiro and G. A. Barbosa, Phys. Rev. A **54**, 3489 (1996).
[4] T. B. Pittman, D. V. Strekalov, D. N. Klyshko, M. H. Rubin, A. V. Sergienko, and Y. H. Shih, Phys. Rev. A **53**, 2804 (1996).
[5] G. A. Barbosa, Phys. Rev. A **54**, 4473 (1996).
[6] E. J. S. Fonseca, P. H. S. Ribeiro, S. Padua, and C. H. Monken, Phys. Rev. A **60**, 1530 (1999).
[7] A. Gatti, E. Brambilla, L. A. Lugiato, and M. I. Kolobov, Phys. Rev. Lett. **83**, 1763 (1999).
[8] A. F. Abouraddy, M. B. Nasr, B. E. A. Saleh, A. V. Sergienko, and M. C. Teich, Phys. Rev. A **63**, 063803 (2001).
[9] B. E. A. Saleh, A. F. Abouraddy, A. V. Sergienko, and M. C. Teich, Phys. Rev. A **62**, 043816 (2000).
[10] G. Brida, E. Cagliero, G. Falzetta, M. Genovese, M. Gramegna, and E. Predazzi, Phys. Rev. A **68**, 033803 (2003).
[11] A. Gatti, E. Brambilla, and L. A. Lugiato, Phys. Rev. Lett. **90**, 133603 (2003).
[12] S. P. Walborn, M. O. T Cunha, S. Padua, and C. H. Monken, Phys. Rev. A **65**, 033818 (2002).
[13] V. Giovannetti, S. Lloyd, and L. Maccone, Phys. Rev. A **65**,

022309 (2002).
[14] A. N. Boto, P. Kok, D. S. Abrams, S. L. Braunstein, C. P. Williams, and J. P. Dowling, Phys. Rev. Lett. **85**, 2733 (2000).
[15] G. Bjork, L. L. Sanchez-Soto, and J. Soderholm, Phys. Rev. A **64**, 013811 (2001).
[16] G. Bjork, L. L. Sanchez-Soto, and J. Soderholm, Phys. Rev. Lett. **86**, 4516 (2001).
[17] M. D. Angelo, M. V. Chekhova, and Y. H. Shih, Phys. Rev. Lett. **87**, 013602 (2001).
[18] A. F. Abouraddy, B. E. A. Saleh, A. V. Sergienko, and M. C. Teich, Opt. Express **9**, 498 (2001).
[19] A. F. Abouraddy, B. E. A. Saleh, A. V. Sergienko, and M. C. Teich, Phys. Rev. Lett. **87**, 123602 (2001).
[20] R. S. Bennink, S. J. Bentley, and R. W. Boyd, Phys. Rev. Lett. **89**, 113601 (2002).
[21] R. S. Bennink, S. J. Bentley, R. W. Boyd, and J. C. Howell, Phys. Rev. Lett. **92**, 033601 (2004).
[22] M. D. Angelo, and Y. H. Shih, e-print quant-ph/0302146.
[23] A. Gatti, E. Brambilla, M. Bache, and L. A. Lugiato, Phys. Rev. Lett. **93**, 093602 (2004).
[24] A. Gatti, E. Brambilla, M. Bache, and L. A. Lugiato, Phys. Rev. A **70**, 013802 (2004).
[25] J. Cheng and S. Han, Phys. Rev. Lett. **92**, 093903 (2004).
[26] A. Valencia, G. Scarcelli, M. D. Angelo, and Y. Shih, Phys. Rev. Lett. **94**, 063601 (2005); quant-ph/0404078.
[27] D. Magatti, F. Ferri, A. Gatti, M. Bache, E. Brambilla, and L. A. Lugiato, quant-ph/0408021.
[28] Y. Cai and S. Zhu, Opt. Lett. **29**, 2716 (2004).
[29] S. A. Collins, J. Opt. Soc. Am. **60**, 1168 (1970).
[30] J. T. Foley and M. S. Zubairy, Opt. Commun. **26**, 297 (1976).
[31] D. Zhang, X. Chen, Y. Zhai, and L. Wu, quant-ph/0503122.